J. Phys. Chem. B **2004,** *108,* 13370−13378

Solvent Polarity across Weakly Associating Interfaces

William H. Steel,[†] **Yuen Y. Lau,**[†] **Carmen L. Beildeck,**[†] **and Robert A. Walker***[,†,‡]

Department of Chemistry and Biochemistry, University of Maryland,
College Park, College Park, Maryland 20742

Received: January 13, 2004; In Final Form: June 16, 2004

Molecular ruler surfactants, solvatochromic probes of solvent polarity, have been used to examine changes in solvent polarity across weakly associating liquid/liquid interfaces. The water/alkane interfaces were formed between an aqueous subphase and either cyclic (cyclohexane and methylcyclohexane) or linear (octane and hexadecane) alkanes. Resonance-enhanced second-harmonic generation was used to collect effective excitation spectra of species adsorbed to these interfaces. As surfactants lengthened, the surfactant probe sampled an increasingly nonpolar environment as evidenced by an excitation wavelength that shifted toward the alkane limit. Data suggest that all four water/alkane interfaces are molecularly sharp (<9 Å), but that differences in the solvent molecular structure alter the transition from aqueous to organic solvation across the interface. Polarity across two interfaces (cyclohexane and hexadecane) changes gradually over the distance spanned by ruler surfactants. In contrast, the transitions at the interfaces between water and methylcyclohexane and octane appear much more abrupt. These findings appear to correlate with each organic solvent's ability to pack and associated free volume. More free volume in the organic phase leads to a more abrupt water/alkane interface. Results are interpreted on the basis of recent molecular dynamics simulations examining polarity at different water/monolayer interfaces.

I. Introduction

At ambient pressure and temperature, oil and water tend not to mix. These boundaries between two immiscible liquids have been the subject of increasing scrutiny during the past decade due to their roles in solvent extraction,[1,2] phase transfer catalysis,[1,2] and environmental remediation.[3] Furthermore, liquid/liquid interfaces frequently serve as biomimetic models of cell membranes[4,5] and are used to guage anaesthetic efficacy[6] as well as protein binding affinity.[4] Numerous experimental and computational techniques have been used to examine how the asymmetry inherent to interfaces affects interfacial structure and long-range order.[7−9] In addition, many of the same methods have been employed to identify how surface-mediated solvent properties change interfacial solvation from bulk solution limits.[10−13] Here, solvation refers to the noncovalent interactions experienced between a solute and its surroundings. Understanding how interfaces alter solute−solvent interactions from those in bulk solution is essential for formulating quantitative, predictive models of solution phase surface chemistry.

In bulk solution a solute is subject to isotropic forces, and continuum models of solvation can accurately describe solute behavior. At an interface, however, solutes experience an anisotropic environment, especially if the solute contains both polar and nonpolar functional groups that lead to surface-induced, polar ordering. Under these circumstances, short-range interactions between a solute and its interfacial surroundings can lead to dramatic changes in solute energetics, structure, and reactivity. In the studies described below, we use second-order nonlinear optical spectroscopy to measure solvent polarity across weakly associating liquid/liquid interfaces. The interfaces all consist of an aqueous phase in contact with an alkane, and the solutes are solvatochromic probes that have been integrated into surfactants of varying lengths, e.g., "molecular rulers".[14,15] Results show that despite having similar bulk dielectric properties, the alkanes create very different dipolar environments at the interface depending on molecular structure.

One of the most fundamental properties associated with liquid/liquid interfaces is one of interfacial width. Across liquid/liquid interfaces, properties such as density, dielectric constant, and refractive index are changing on some length scale. This distance may be short by molecular standards, leading to abrupt changes in these solvent properties, or interfacial width may be broad with properties changing gradually over multiple solvent diameters. The most direct measure of interfacial width comes from X-ray and neutron scattering studies. These experiments explicitly identify the distance across which solvent density changes. X-ray scattering studies of different water/alkane interfaces show these boundaries to be molecularly sharp,[16] in agreement with predictions based on capillary wave theory[7] as well as molecular dynamics simulations.[17] However, these data do not probe the interactions between a solute and its surroundings. Similarly, neutron scattering studies have identified how liquid/liquid interfaces induce gradients in interfacial salt concentrations and control the structure of adsorbed surfactants,[18] but again, results identify the distribution of species across an interface, not the forces between them.

Optical spectroscopy cannot measure the spatial or distance-dependent information necessary for determining interfacial width, but optical spectroscopy *does* measure solvation forces directly. When coupled with methods to ensure surface specificity, i.e., a total internal reflection geometry or a second-order nonlinear response, fluorescence and nonlinear optical spectroscopy can serve as a versatile means for probing interfacial solvation across a variety of liquid/liquid interfaces. For example, using rotational anisotropy of a solute's fluorescence

---

[†] Department of Chemistry and Biochemistry.

[‡] Chemical Physics Program.

10.1021/jp0498318 CCC: $27.50 © 2004 American Chemical Society
Published on Web 08/11/2004

Wirth and co-workers demonstrated that interfacial viscosity depended sensitively on solvent structure in ways that could not be predicted on the basis of bulk viscosity values.[19−21] Similarly, Eisenthal and co-workers employed resonance-enhanced second-harmonic generation to show that solute isomerization rates at interfaces varied depending on the phase in which the solute was actually solvated.[22,23] More recently, these techniques have been used to examine electron and energy transfer between interfacial species to infer how surface effects alter interfacial solvation from solvation in bulk solution.[12,24] Several of these studies suggest that liquid/liquid interfaces are molecularly sharp, but quantitative data about interfacial width remain elusive.

Of particular relevance to the work described below are a series of studies by Wang et al. that probed interfacial polarity at a number of liquid/liquid and liquid/vapor interfaces.[22,23] In these experiments, second harmonic generation (SHG) was used to acquire effective excitation spectra of solvatochromic solutes adsorbed on the different system surfaces. The probes themselves had excitation wavelengths that varied considerably depending on whether the probe was solvated in a polar or nonpolar medium. Data showed that interfacial polarity could be described by an average polarity model in which the local dielectric environment contained approximately equal contributions from both bulk phases. This model can be described remarkably well by continuum-based scales of solvent polarity. At first, this result may seem surprising in light of the X-ray scattering experiments that show liquid/liquid interfaces to be molecularly sharp.[16] One might expect interfacial polarity to reflect disproportionate contributions from one phase or the other. However, in a series of molecular dynamics simulations Michael and Benjamin showed how a molecularly sharp interface could give rise to the average polarity picture if the interface was thermally roughened and the solute resided very close to the Gibbs dividing surface.[17] These simulations also suggested that results should be very sensitive to solute distribution across the interface, a conclusion that was later supported by additional SHG experiments.[13,25]

II. Experimental Section

Experiments described in this work couple resonance-enhanced SHG spectroscopy with surfactants created specifically to vary the equilibrium distribution of solvatochromic solutes across a liquid/liquid interface. By measuring how SHG spectra vary with surfactant length, the dipolar width of different weakly associating liquid/liquid interfaces has been measured. The alkanes used to create an interface with an aqueous subphase include cyclohexane, methylcyclohexane, octane, and hexadecane. All of these interfaces appear to be molecularly sharp; namely, solvent polarity converges to bulk alkane limits on subnanometer length scales, but there exist qualitative differences between the different systems that cannot be described by differences in bulk solvent properties. These findings are discussed in terms of the molecular structure of the individual solvents themselves and recent simulations that expose the role of interfacial roughness on solvation dynamics and interfacial polarity.

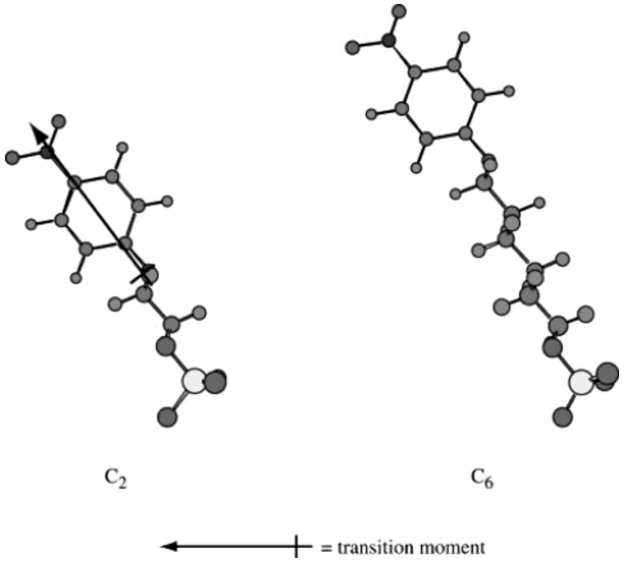

Figure 1. Structures of two of the molecular ruler surfactants used in this work. The notation C_n denotes the number of methylene groups (n) separating the sulfate headgroup from the aromatic, PNAS-based chromophores. The structures shown in this figure correspond to surfactants having 2 (C_2) and 6 (C_6) methylene groups. Shown on the C_2 chromophore is the direction of the electronic transition moment corresponding to the S_1-S_0 electronic excitation sampled by the resonance-enhanced SHG measurements. The transition moments of the chromophores are aligned ~40° off of what would be the surface normal of the liquid/liquid interfacial systems discussed in this work.

Molecular rulers are surfactants containing an ionic headgroup attached to a hydrophobic nitrobenzene chromophore via an alkyl spacer whose length can be varied by controlling the number of methylene groups present. They are synthesized via a moderately simple two-reaction process. A 1,*n*-diol containing the number of methylene groups desired in the spacer of the final surfactant is combined with *p*-fluoronitrobenzene to produce an intermediate product containing a terminal alcohol. The alcohol is converted to an ionic sulfate group by the addition of chlorosulfonic acid. Surfactants have been produced with spacers ranging from two to eight methylene groups, primarily in even increments. A more complete description of synthetic conditions can be found in ref 14, and representative structures of C_2 (2 methylene groups) and C_6 (6 methylene groups) surfactants appear in Figure 1.

After ruler surfactants had been synthesized and purified, their solvatochromic behavior and surface activity were characterized. By measuring the excitation maxima (λ_{max}) of the family of molecular rulers in a variety of solvents having different polarities we concluded that their solvatochromic behavior closely matches that of the model chromophore, *para*-nitroanisole (PNAS). PNAS is an ideal probe for the study of interfacial polarity for a number of reasons. It contains a single chromophoric benzene ring, meaning experiments detect signal from a single source, rather than the averaged signal from multiple chromophores that are present in a number of dyes used in previous studies of interfacial polarity. PNAS exhibits a single electronic excitation in the wavelength region between 270 and 350 nm. This excitation is accompanied by a large change in the molecule's permanent dipole. As a result, PNAS has a broad solvatochromic window: its excitation maximum red shifts by more than 20 nm from its value in nonpolar, organic solvents to that in water. Finally, PNAS contains a polar nitro group and a nonpolar methoxy group, imparting an affinity for both the polar and nonpolar solvent phases at water/alkane interfaces.

The Wilhelmy plate method was used to measure the surface activity of different length molecular rulers at different water/alkane interfaces. From these data, using procedures described in ref 14, terminal surface concentrations ranged from 1.5×10^{14} to 1.9×10^{14} molecules/cm^2 for different length molecular rulers. Surface activities of two neutral chromophores used in SHG studies were also measured. PNAS was found to have a terminal surface concentration of only 4.1×10^{13} molecules/

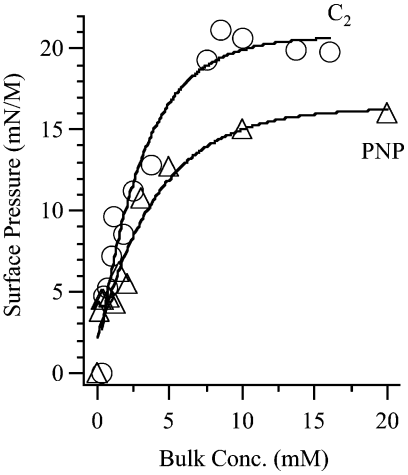

Figure 2. Representative surface pressure isotherms for C_2 rulers (circles) and PNP (triangles) adsorbed to a water/cyclohexane interface. Other water/alkane interfaces led to quantitatively similar isotherms. Interfacial tensions were collected using the Wilhelmy plate method for these species and others studied in this work. From these isotherms, terminal surface concentrations can be determined as described in ref 14. Note that SHG experiments described in this work all involve aqueous concentrations of less than 2 mM, leading to surface coverages of less than 20% of full monolayer coverage.

TABLE 1: Partitioning Results of PNP and PNAS in Several Water/Alkane Systems Characterized as Ratio of Concentrations of Solute in Each Phase

solute	system	partitioning ratio (water:organic)
PNP	water:cyclohexane	113 ± 10:1
PNP	water:m-cyclohexane	104 ± 10:1
PNP	water:octane	121 ±20:1
PNP	water:hexadecane	42 ± 5:1
PNAS	water:cyclohexane	1:23 ± 5
PNAS	water:octane	1:18 ± 5

cm^2 at the water/cyclohexane interface. As expected, *para*-nitrophenol (PNP) was found to be more surface active at weakly associating water/alkane interfaces, forming monolayers with terminal surface concentrations between 1.9×10^{14} and 2.4×10^{14} molecules/cm^2. Both of the neutral species were found to be excellent probes of solvation at water/alkane interfaces. Representative surface pressure isotherms for C_2 rulers and PNP are shown in Figure 2.

Motivated by a need to better understand molecular ruler behavior at liquid surfaces, we measured the neutral chromophore partitioning across various weakly associating water/alkane interfaces. Ideally, the solvatochromic probe of molecular ruler surfactants would be hydrophobic enough so that it would solvate itself as much as possible in the lower dielectric, organic phase. Opposing this tendency is the affinity of the polar nitro group for the higher dielectric, aqueous phase, possibly causing the molecular rulers to tilt toward the interfacial plane. As the data in Table 1 show, PNP partitioned to the water layer preferentially. With the exception of the water/hexadecane system, PNP was approximately 100 times more soluble in water than the organic phase. In contrast, PNAS displayed a preference for the organic layer over the aqueous phase, with a partitioning ratio of ~20:1 (organic:aqueous). The chromophore incorporated into ruler surfactants more closely resembles PNAS than PNP; thus we feel confident that at water/alkane interfaces the ruler probe will attempt to solvate itself in the organic phase. (Specific partitioning experiments with the ionic molecular ruler species were not feasible, as the anionic sulfate group prohibits surfactant solvation in the nonpolar, alkane phase.)

Resonance-enhanced SHG was used to acquire effective excitation spectra of molecular rulers adsorbed to different water/alkane, liquid/liquid interfaces. Because of its origins, the resonance-enhanced response is both surface and molecularly specific, meaning that spectra result only from solutes influenced by interfacial anisotropy.[22,26] In a typical experiment, a single coherent optical field of frequency ω is incident upon an interface having a submonolayer coverage of a given ruler surfactant. A nonlinear polarization of frequency 2ω and intensity $I(2\omega)$ is detected, where the intensity of this second harmonic is proportional to the square of the second-order susceptibility, $\chi^{(2)}$,

$$I(2\omega) \propto |\chi^{(2)}|^2 I(\omega)^2 \tag{1}$$

and $\chi^{(2)}$ is a third-rank tensor that under the electric dipole approximation is zero in isotropic environments. The $\chi^{(2)}$ tensor, then, imparts to the technique its inherent surface specificity. The tensor itself contains both resonant and nonresonant contributions:

$$\chi^{(2)} = \chi^{(2)}_{\mathrm{R}} + \chi^{(2)}_{\mathrm{NR}} \tag{2}$$

For dielectric systems, such as the water/alkane interfaces considered here, the resonant term is typically several orders of magnitude larger than the nonresonant contribution and can be related to the microscopic hyperpolarizability:

$$\chi^{(2)}_{\mathrm{R}} = \sum_{\mathrm{k,e}} \frac{\langle \mu_{\mathrm{gk}} \mu_{\mathrm{ke}} \mu_{\mathrm{eg}} \rangle}{(\omega_{\mathrm{gk}} - \omega - \mathrm{i}\Gamma)(\omega_{\mathrm{eg}} - 2\omega - \mathrm{i}\Gamma)} \tag{3}$$

where μ_{ij} is the transition matrix element between state *i* and state *j* (where g stands for the ground state, k for an intermediate, virtual state, and e for the first excited state). The ω_{ij} refer to the transition energies between the ground state and states k and e, and Γ is the transition's line width. When 2ω is resonant with ω_{eg}, $\chi^{(2)}$ becomes large, leading to a strong resonance enhancement in the observed intensity at 2ω. Thus, measuring the scaled intensity $(I(2\omega)/I^2(\omega))$ as a function of 2ω records an *effective* excitation spectrum of solutes adsorbed to an interface in a manner developed first by Eisenthal and co-workers.[22,23] With the exception of data recorded to determine solute orientations, spectra in this work were acquired under $P_\omega P_{2\omega}$ polarization conditions, where P polarized light describes light that is polarized vertically perpendicular to the direction it travels. Varying the incident and detected polarizations enabled us to determine the average chromophore orientation using methods described previously.[13] Different polarizations did not lead to qualitatively different SHG spectra.

To record spectra, aqueous solutions of solutes were prepared between 0.5 and 2 mM. These concentrations lead to surface coverages of less than 20% of a full monolayer according to adsorption isotherms recorded for rulers at the water/cyclohexane and water/octane interfaces. Liquid/liquid interfaces were generated by first placing aqueous solutions into a cylindrical kel-F cell having a reservoir 4 cm in diameter. Then an application of a thin layer (~1−3 mm) of organic solvent atop the aqueous solution creates the aqueous−organic interface. A trapezoidal fused silica prism (50 × 50 × 30 mm, JDSU Casix) is secured atop the reservoir, preventing evaporation of the solvent. Prior to use, the prism is cleaned in a 50:50 mixture (by volume) of concentrated sulfuric and fuming nitric acid. Prisms cleaned in this way have been shown to be hydrophilic, as demonstrated by complete wetting of the surface. All liquid/

liquid interfaces and SH spectra were acquired at room temperature, 22 ± 1.5 °C.

The SHG apparatus is built around a Ti:sapphire regeneratively amplified, femtosecond laser (Clark-MXR CPA 2001) that produces 130 fs pulses with energies of ∼700 μJ at a wavelength of 775 nm and a repetition rate at 1 kHz. The output of the Ti:sapphire laser pumps a commercial optical parametric amplifier (OPA, Clark-MXR). The visible output of the OPA is tunable from 550 to 700 nm, with a bandwidth of 2.5 ± 0.5 nm. The polarization of the incident beam is controlled using a Glan-Taylor polarizer and a half-wave plate. A series of filters block the fundamental 775 nm and any second-harmonic light generated from the preceding optical components. Second-harmonic photons are detected in the reflected direction using photon-counting electronics. Typical signal levels average 0.01−0.1 photon per shot. A second polarizer selects the polarization of the SH signal, and a short pass filter and monochromator serve to separate the second-harmonic signal from background radiation due to scattering and fluorescence.

Because the visible OPA cannot be synchronously tuned, acquisition of a complete SHG spectrum requires multiple hours. A typical procedure entails letting the liquid−liquid system equilibrate followed by manual tuning of ω_{vis} to each desired wavelength. System alignment is reoptimized at every wavelength to account for the wavelength-dependent refractive indices of the prism and collection optics. At each wavelength, SH data are collected for four 10 s intervals and normalized for incident power. Although tedious, this procedure ensures that spectra are reproducible. A single wavelength might be sampled three separate times several hours apart (beginning, middle, and end of an acquisition sequence). If the normalized SH signal from each of these three samples does not fall within experimental uncertainty (typically ±15%), data acquisition is halted and the spectrum discarded. In addition, data at the same wavelength were often acquired using several different incident powers and then normalized to confirm quadratic dependence of SH signal intensity on the incident field intensity predicted by eqs 1−3. Predicted quadratic behavior was always observed.

III. Results

Figure 3 shows the SHG spectra of four different solutes adsorbed to the water/cyclohexane interface: PNAS, C_2 ruler, C_4 ruler, and C_6 ruler. The SH data are fitted with eqs 1−3. Overlaid on the plots are dotted and dashed lines to denote the excitation maxima of each species in bulk and organic aqueous solutions, respectively. (Due to solubility limits of the ionic rulers in alkane solvents, neutral molecular rulers containing a terminal hydroxyl group in place of the ionic sulfate group were used to determine excitation maxima these nonpolar solvents. When maxima for both neutral and ionic species could be collected (in more polar solvents) they were found to be equivalent.) The solid vertical line on each panel indicates the fitted interfacial maximum of each species (including the nonresonant contribution). Note that interference effects between the resonant and nonresonant contributions to $\chi^{(2)}$ can lead to a calculated SH maximum that does not coincide with the apparent spectral maximum. (For example, see the bottom panel of Figure 3, depicting the SHG spectrum of the C_6 ruler at the water/cyclohexane interface.)

Data clearly show that the chromophores of each ruler species experience unique solvation environments. The transition maximum for PNAS at the water/cyclohexane interface is 309 ± 2 nm, compared to its bulk water and organic limits of 316 and 294 nm, respectively. This result is close to the energetic arithmetic mean of the aqueous and organic limits and is consistent with previous studies of interfacial polarity across different weakly associating interfaces.[23] As the chromophore of each subsequent species is allowed to “float” into the organic solvent by lengthening the ruler chain, we observe dramatic changes in the measured transition maximum and excitation bandwidth. The chromophore experiences an increasingly nonpolar environment as the alkyl spacer lengthens from C_2 to C_4 to C_6. This nonpolar environment is reflected by an excitation wavelength that blue shifts from 302 nm (C_2) to 296 nm (C_6). The bulk solution limits of these ruler species are 318 ± 2 nm in water and 295 ± 2 nm in cyclohexane. In earlier work, we attributed these results to a gradual convergence of the local dielectric character to the organic limit.[13] The alkyl spacer separating the chromophore from the ionic headgroup of the C_6 ruler has a maximum length of 9 Å, or approximately three water diameters. This value reflects an upper limit to the interfacial dipolar width and would decrease if there were conformational defects in the alkyl spacers or a net tilt of the adsorbed surfactant. Experiments examining the orientation of adsorbed molecular rulers suggest that—on average—disorder in alkyl chains is not an issue with rulers of increasing length.[14] Given laser spot sizes of ∼100 μm and surface concentrations of ∼10^{13}/cm^2, results necessarily reflect the ensemble averages of ∼10^9 adsorbed surfactants.

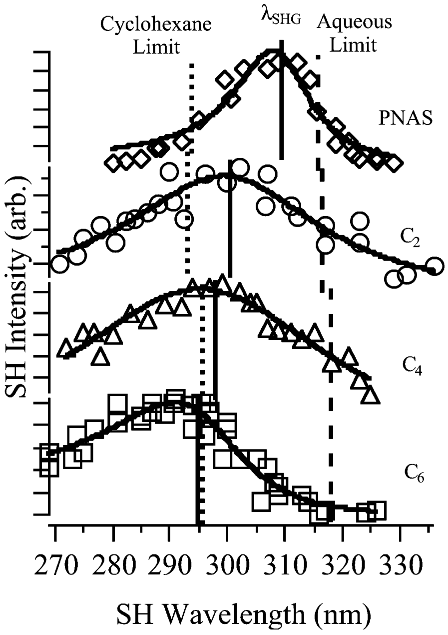

Figure 3. Resonance-enhanced SHG spectra of (top to bottom) *p*-nitroanisole (PNAS), C_2 rulers, C_4 rulers, and C_6 rulers adsorbed to a water/cyclohexane interface. Dotted and dashed vertical lines denote excitation maxima in bulk cyclohexane and water, respectively. Solid vertical lines correspond to SHG maxima (λ_{SHG}) as determined by fitting the data to eqs 1−3. Note that SHG maxima do not always correspond to the wavelengths with the highest SHG intensity, owing to the nonresonant contribution to $\chi^{(2)}$ in eq 2.

A second striking feature that stands out in the four spectra is the marked change in line width as the length of the alkyl spacer increases. In bulk solution, the full-width, half-maximum (fwhm) of the excitation spectrum varies between approximately 44 nm in cyclohexane and 68 nm in water. In a given solvent, excitation bandwidths of different species (e.g., C_2, C_4, C_6, etc.) vary by less than 10%. While there is little variation in the measured line width of each bulk solution spectrum, the interfacial spectra are marked by dramatic changes in their widths. The fwhm of the PNAS spectrum is 15 nm, the sharpest

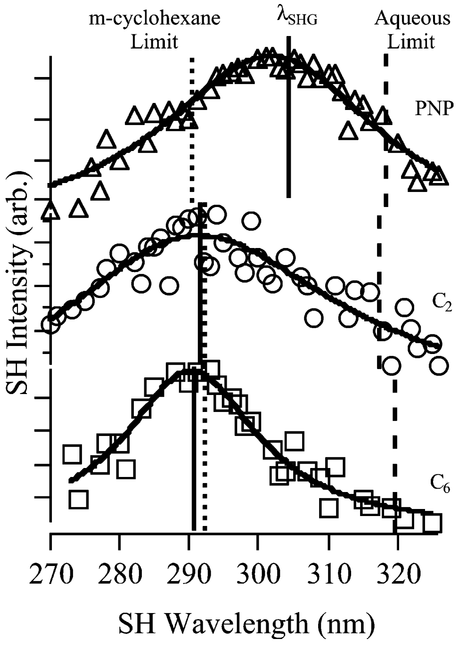

Figure 4. Resonance-enhanced SHG spectra of (top to bottom) *p*-nitrophenol (PNP), C_2 rulers, and C_6 rulers adsorbed to a water/m-cyclohexane interface. Dashed, dotted, and solid vertical lines have the same significance as in Figure 2.

of the four species. This value increases for the C_2 and C_4 rulers, to 39 and 52 nm, respectively, before decreasing to a line width of 25 nm for the C_6 ruler. Interfacial line widths that are narrower than bulk solution limits imply a more homogeneous distribution of solvation environments at the interface relative to bulk solution. Narrow line widths are expected given that chromophores at liquid/liquid interfaces are "anchored" to the boundary by the ionic headgroup and should share a common "float depth" and average orientation. Thus we would interpret line width changes to indicate that the chromophores of the C_2 and C_4 rulers experience a more heterogeneous environment in the interfacial region, possibly due to the influence of capillary wave action. Thermal roughening of the interface would influence the solvatochromic response of shorter surfactants more so than longer surfactants due to proximity effects. The consequence of thermal roughening of the interface would be broader spectra from C_2 surfactants and narrower spectra from the C_6 (and C_8) species.

Figure 4 shows the SH spectra of three species adsorbed to the water/methylcyclohexane (m-cyclohexane) interface. We have probed chromophore excitation at the liquid/liquid interface using PNP and the C_2 and C_6 rulers. As in the water/cyclohexane case, the dashed and dotted lines denote the excitation maxima of the species in bulk water and m-cyclohexane, respectively. Again, the neutral species, PNP in this case, experiences an interfacial polarity that is intermediate between the aqueous and organic limits. The fitted excitation maximum of 304 nm represents the energetic average of the water and m-cyclohexane limits of 318 and 290 nm, respectively. However, unlike at the water/cyclohexane interface, the C_2 ruler experiences a local polarity that is equivalent to that of bulk m-cyclohexane. The chromophore of the C_6 ruler also experiences bulk organic-like solvation at this interface. The only significant difference between the C_2 and C_6 spectra is the line widths of the SHG features. This quantity decreases from 46 nm for the C_2 ruler to 22 nm for the C_6 ruler, again implying that the probe of the shorter surfactant experiences a more heterogeneous environment than the probe of the longer surfactant.

Despite similarities in the spectral line widths from the water/cyclohexane and water/m-cyclohexane systems—C_2 spectra are broad, C_6 spectra are narrow—the solvatochromic responses of molecular rulers adsorbed to these two interfaces show clear differences in interfacial polarity. Polarity changes gradually across the water/cyclohexane interface, but this transition appears much more abrupt at the water/m-cyclohexane interface. In fact, a C_2 ruler separates headgroup and chromophore by ~3 Å, *or less than one water diameter*! Despite this short separation from a headgroup that can only be solvated in the aqueous phase, the chromophore of a C_2 ruler samples an alkane-like, low-polarity environment at the water/m-cyclohexane interface.

This comparison represents the first experimental evidence that a slight alteration of organic solvent structure results in a quantitatively sharper liquid/liquid interface. The dramatic difference between the two systems is somewhat surprising, considering the similarities between bulk cyclohexane and m-cyclohexane. Both solvents have similar dielectric constants (2.0), bulk excitation maxima for the C_2 ruler (293 nm), densities (0.770 and 0.779 g/mL, respectively), and indices of refraction (1.426 and 1.422, respectively). Additionally, the solubility of water in cyclohexane is very similar to that in m-cyclohexane, approximately 0.012 wt % at 20 °C.[27]

One possible source of the observed difference between the systems might arise from differences in the orientation of adsorbed chromophores with respect to each interface. Polarization-dependent SHG measurements have been used to determine the average orientation of the chromophore relative to the surface normal in a manner similar to that described in ref 30. For similar concentrations of C_2 ruler at the water/cyclohexane and water/m-cyclohexane interfaces, the chromophore adopts different orientations. At the water/m-cyclohexane interface the pseudo C_2 axis of the C_2 chromophore is oriented approximately 37° off the interfacial normal, while at the water/cyclohexane interface the pseudo C_2 axis is tilted further off-axis (47°). This difference leads to a difference in the projection of the PNAS transition moment onto the surface normal. Assuming the PNAS chromophore to be ~7 Å long, these tilt angles lead to projections that differ by ~1 Å (5.5 Å at the water/m-cyclohexane interface and 4.5 Å at the water/cyclohexane interface). In other words, at the water/cyclohexane interface the molecular ruler chromophore is more susceptible to the solvating influence of the adjacent aqueous phase. A difference of 1 Å may seem quite small, but previous experimental studies and simulations of solvation at weakly associating liquid/liquid interfaces have shown that even small changes in a solute equilibrium distribution can have a dramatic effect on the resulting solvation experienced by the solute.[25,28] At the water/m-cyclohexane interface the more upright geometry may expose the chromophore to a more alkane-like environment, while at the water/cyclohexane interface the chromophore may remain more readily solvated by water. The net result is that the water/m-cyclohexane interface has a more abrupt transition from bulk water to alkane than the water/cyclohexane interface.

In principle, one might expect such abrupt changes in environment to reflect themselves in SH experiments carried out under different polarization conditions (i.e., $M_{in}S_{out}$ or $P_{out}S_{in}$) with the largest differences to appear for C_2 rulers that localize chromophores closest to the nominal interfacial boundary. However, the C_2 spectra are consistently twice as broad as spectra acquired using longer surfactants (fwhm ~50 nm) and thus do not afford us the sensitivity to discern variation in the "in-plane" versus "out-of-plane" polarity. In spectra where the

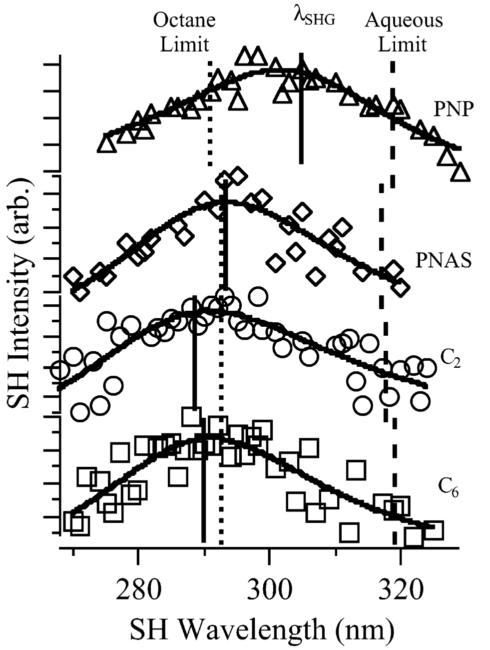

Figure 5. Resonance-enhanced SHG spectra of (top to bottom) PNP, PNAS, C_2 rulers, and C_6 rulers adsorbed to a water/octane interface. Dashed, dotted, and solid vertical lines have the same significance as in Figure 2.

lines are sharper (and the surfactant lengths longer), invariance in spectra may be attributed to a homogeneous dielectric environment (for an anisotropic distribution of chromophores).

Results similar to those from the water/m-cyclohexane interface are observed at the water/octane interface. Figure 5 shows the SH spectra of PNP, PNAS, C_2 ruler, and C_6 ruler at the water/octane interface. Again, the dotted and dashed lines indicate the excitation maxima of each species in bulk water and octane. We see from the PNP spectrum that the chromophore experiences a surrounding solvation that appears to represent averaged contributions from the two adjacent solvent layers. Just as in the water/m-cyclohexane system we observe a striking transition to an alkane-like dielectric environment with very short molecular rulers. In fact, even the neutral PNAS chromophore experiences an environment suggesting bulk octane solvation. Subsequent spectra of the C_2 and C_6 rulers indicate that these species, too, experience an octane-like solvation. While the spectra indicate that each chromophore samples a low-polarity environment, the interfacial line width of the C_2 spectrum is much broader, 50 nm, than that of the C_6 spectrum, 28 nm. The data suggest that although the chromophores of both ionic ruler surfactants are surrounded by an alkane environment, the C_2 ruler chromophore experiences a less homogeneous environment at the water/octane interface than the C_6 ruler chromophore.

In each of the previous systems discussed (and the system to follow), interfacial solvation of the adsorbed neutral chromophores generally reflected averaged contributions from the two adjacent solvent phases. One might be surprised, then, that PNAS experiences an octane-like solvation at the water/octane interface. The change from a hydrophilic hydroxyl group (PNP) to a hydrophobic methoxy group (PNAS) alters the overall hydrophobic/hydrophilic balance in two solutes that otherwise share similar solvation behavior. Water/octane partitioning data were collected for both PNP and PNAS and are shown in Table 1. We observed that PNP partitioned to the aqueous phase relative to the organic phase with an equilibrium constant of more than 100. Conversely, PNAS preferentially partitioned to the octane layer by a ratio of almost 20:1 (octane:water), a difference in K_{eq} of more than 3 orders of magnitude. PNAS, then, is more likely to be solvated by octane molecules at the water/octane interface, accounting for the rapid transition to the nonpolar solvation reported by the bare, adsorbed PNAS chromophores. Similar behavior has been observed previously and predicted by simulation.[25,28] This observation emphasizes that subtle variations in solute structure can impact significantly the equilibrium distribution of solutes across interfaces, leading to markedly different local environments experienced by solutes *at the same interface*.

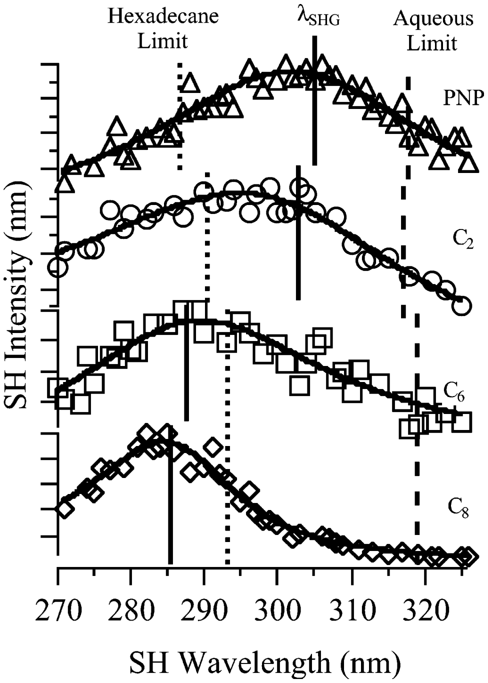

Figure 6. Resonance-enhanced SHG spectra of (top to bottom) PNP, C_2 rulers, C_6 rulers, and C_8 rulers adsorbed to a water/hexadecane interface. Dashed, dotted, and solid vertical lines have the same significance as in Figure 2.

Additionally, we might expect that because PNAS exhibits an increased affinity for the organic phase, the molecules will be drawn more into the organic layer, thus adopting a more upright orientation with respect to the interfacial plane. Polarization-dependent SHG measurements were collected for PNP and PNAS at the water/octane interface and indicate that PNP is tilted 49° off normal, while PNAS leans only 34° off normal, a significant difference. The PNAS adopts a more upright orientation, meaning the chromophore is more effectively solvated by the organic phase than is PNP. Presumably, the structure of PNP induces the molecule to lie further off of the surface normal in order to solvate both polar functional groups.

The SHG spectra in Figure 6 show the behavior of PNP, C_2 rulers, C_6 rulers, and C_8 rulers adsorbed to the water/hexadecane interface. The data are not as clean as in other weakly associating systems, raising some concerns about our interpretation. Specifically, the C_2 and C_6 ruler spectra are noteworthy because they contain large nonresonant contributions that shift the spectral maxima far from the observed intensity maxima and cause the intensity to “leak” to shorter wavelengths in the C_2 ruler spectrum and to longer wavelengths in the C_6 ruler spectrum. Two sources could account for the observed distortions on the SH spectra: a large nonresonant term or a broad distribution of local environments (leading to extreme inhomogeneous broadening). The origins of this large nonresonant contribution are not immediately clear, yet the return to a well-defined spectrum for the C_8 ruler makes us confident that these spectra represent real behavior of ruler surfactants adsorbed to the liquid/liquid interface.

Examining the fitted intensity maxima of the series of spectra, we observe that the neutral chromophore experiences a local polarity that is intermediate between the two bulk limits. In contrast to the behavior observed at the water/octane interface, the C_2 ruler also reflects such intermediate solvation. The excitation wavelength maximum of the C_2 ruler at the water/hexadecane interface is 303 nm. The spectrum of the C_6 ruler is fitted to an interfacial maximum of 290 nm, which indicates a polarity slightly lower than that of the C_6 ruler in bulk hexadecane (294 nm). Unlike at the three previous interfaces, the C_6 ruler spectrum at the water/hexadecane interface is broad (43 nm) and comparable to the line widths of 42 and 50 nm for PNP and the C_2 ruler at this interface. We see in the bottom panel of Figure 6 that the C_8 ruler spectrum is much sharper (fwhm = 23 nm) and reflects a transition maximum of 286 nm, a curious value because it would indicate a surrounding solvation that is much less polar than bulk hexadecane. The line width data suggest that solutes sample a broader distribution of environments at the water/hexadecane interface than at other weakly associating interfaces.

IV. Discussion

A common feature of the weakly associating interfaces examined in this work is that they are all molecularly sharp: in each case the solvatochromic probe of the C_6 ruler experiences a solvation representative of the bulk organic solvent. This sets an upper limit on the dipolar width of these weakly associating interfaces; as previously mentioned, a fully extended C_6 spacer oriented perpendicular to the interface stretches 9 Å between the oxygen on the chromophore and the oxygen on the sulfate headgroup. However, qualitative differences do exist between the four alkane/water interfaces studied. The transition to bulk alkane solvation across the water/cyclohexane and water/hexadecane interfaces is more gradual than it is across the water/m-cyclohexane and water/octane interfaces. This behavior is evidenced by two experimental observables, excitation wavelength and spectral line width. Figures 7 and 8 summarize wavelength and line width data for different length rulers adsorbed to different water/alkane interfaces. In Figure 7 the decrease in excitation wavelength is more gradual at the water/cyclohexane and water/hexdecane interfaces and more abrupt at the water/m-cyclohexane and water/octane interfaces. Figure 8 demonstrates that the shorter interfacial probes produce broader spectral bands and that the longest probe used to examine each system always produced the narrowest line width. To further clarify these trends, a summary table including interfacial SHG maxima, line width, and orientation data for the species and interfaces discussed appears in Table 2.

Any analysis of the differences arising at different water/alkane interfaces should begin by considering the different molecular structures of the alkanes. Of the alkane solvents used in these studies, two are cyclic (cyclohexane and m-cyclohexane) and two are linear (octane and hexadecane). Within each pairing the molecular ruler data suggest that one interface is sharper than the other. In this section, we will examine different factors that can influence interfacial width and speculate on the origins of the observed differences.

1. Cyclic Alkanes. In the case of the cyclic solvents, spectra in Figures 3 and 4 (and data in Figures 7 and 8) indicate that the water/m-cyclohexane interface is sharper than that of the water/cyclohexane system. On the basis of solvent packing considerations and attractive intermolecular forces—cyclohexane has a smaller surface area and molecular volume and higher melting point than m-cyclohexane—intuition might lead one to guess the opposite to be true. Cyclohexane experiences stronger intermolecular interactions and greater long-range order than

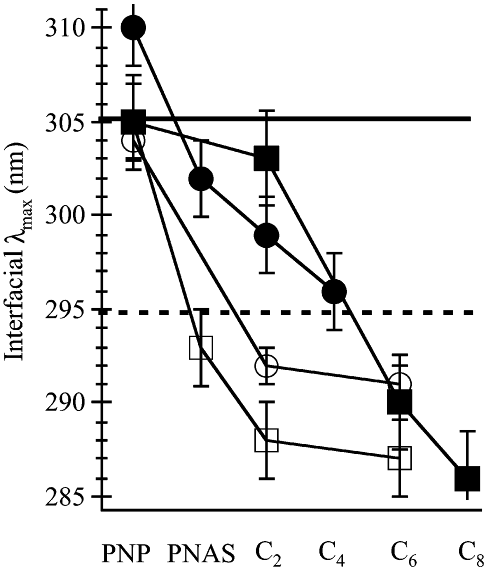

Figure 7. Fitted interfacial SHG maxima for species adsorbed to weakly associating liquid/liquid and water/alkane interfaces. The dashed horizontal line denotes the average excitation wavelength of the species in bulk organic solvents (~295 nm). The solid horizontal line denotes the energetic average of the aqueous and organic excitation wavelengths. Two of the interfaces feature a gradual transition from an average polarity to a bulk organic polarity: cyclohexane (filled circles) and hexadecane (filled squares). Two interfaces have abrupt transitions from average polarity to bulk organic solvation: m-cyclohexane (open circles) and octane (open squares).

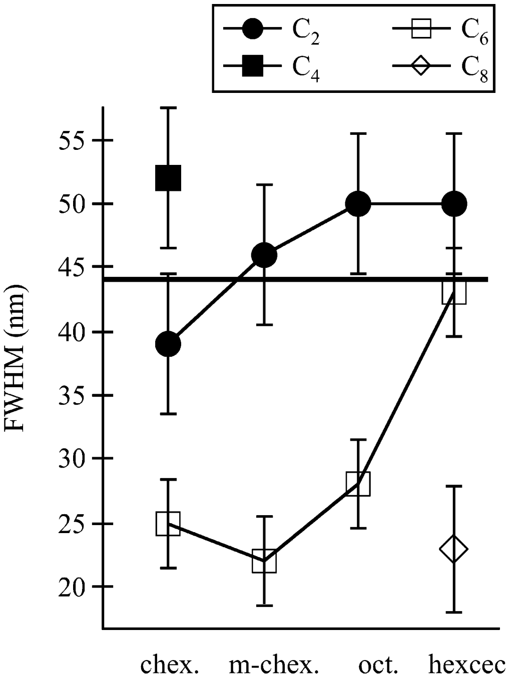

Figure 8. Line width data for SHG spectra of molecular rulers adsorbed to liquid/liquid interfaces between water and cyclohexane, m-cyclohexane, octane, and hexadecane. The horizontal line denotes the average line width of excitation spectra of molecular rulers in bulk organic solvents (~44 nm). The four species shown include C_2 (filled circles), C_4 (filled squares), C_6 (open squares), and C_8 (open diamond). At each interface the longest species produced the spectrum with the narrowest line width.

TABLE 2: Summary of Data Collected for Species Adsorbed to Liquid/Liquid Water/Alkane Interfaces[a]

solute	organic solvent	interfacial max. (nm)	fwhm (nm)	tilt angle (deg)
PNP	cyclohexane	310	33	53
PNAS	cyclohexane	309	15	
C_2 ruler	cyclohexane	302	39	47
C_4 ruler	cyclohexane	299	52	51
C_6 ruler	cyclohexane	296	25	45
PNP	m-cyclohexane	304	35	42
C_2 ruler	m-cyclohexane	292	46	37
C_6 ruler	m-cyclohexane	291	22	44
PNP	octane	305	42	49
PNAS	octane	293	44	34
C_2 ruler	octane	288	50	42
C_6 ruler	octane	287	28	
PNP	hexadecane	305	42	44
C_2 ruler	hexadecane	303	50	
C_6 ruler	hexadecane	290	43	43
C_8 ruler	hexadecane	286	23	

[a] The average excitation wavelength of species is ~295 nm in bulk organic solvents and ~318 nm in bulk water. Interfacial max. refers to the fitted excitation maximum as determined by fitting spectra with eqs 1−3. Full-width half-maximum (fwhm) describes the line width of SHG spectra collected at liquid/liquid interfaces. Tilt angle refers to the orientation of the species chromophore at liquid/liquid interfaces relative to surface normal.

m-cyclohexane. Thus we might expect cyclohexane to become more ordered at the water/cyclohexane interface, leading to an abrupt transition from an aqueous solvation environment to an organic limit. In contrast, m-cyclohexane would be more disordered adjacent to a water boundary, and one might anticipate a more gradual transition from the aqueous to organic limit. However, solvation across liquid/liquid interfaces will not necessarily reflect bulk solution properties, and there exist several considerations that contradict bulk solvent-based intuition and, instead, support findings presented here.

Theoretical and statistical models of interfaces express the interfacial width as the combination of an intrinsic profile width and a capillary wave contribution that is inversely proportional to the surface tension of the interface.[29] The water/cyclohexane interfacial surface tension is 50.2 mN/m, while the water/m-cyclohexane has an interfacial tension of 51.5 mM/m as measured with the Wilhemy plate method in our lab. The higher surface tension for the water/m-cyclohexane interface implies a smaller capillary wave contribution to surface roughness and thus a narrower interfacial region separating bulk water from bulk alkane. This interpretation should be viewed cautiously, however, given that Schlossman and co-workers found that the capillary wave contribution was fairly constant across a broad range of water/alkane interfaces having interfacial tensions that varied by more than 3 mN/m.[7]

Of greater significance to our interpretation are a series of molecular dynamics simulations of water/alkane interfaces performed by Vieceli and Benjamin. In these simulations the authors varied interfacial properties between water and an alkane monolayer by altering the length of the alkane chains present and attaching chlorine atoms to some or all alkanes. In doing so they generated a series of interfaces having varying character: smooth or rough; methyl-terminated, chlorine-terminated, or mixed. The interface could also be varied in terms of whether the terminal methyl group or chlorine atom (when present) was “in” or “out” with respect to the interfacial plane. The local environment was then examined by placing a dipolar probe at each interface and evaluating different contributions to the probe’s solvation energy. (Figure 9 shows a schematic representation of these interfacial topographies.) The simulations generated electronic absorption spectra of the probe molecule at these interfaces and therefore serve as a useful guide for interpreting our studies of solute excitation at liquid/liquid interfaces. Vieceli and Benjamin were able to summarize the polarity of their series of methyl-terminated interfaces as follows:

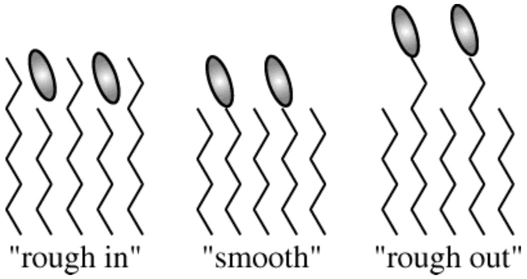

Figure 9. Schematic representation of three liquid/monolayer interfaces simulated by Vieceli and Benjamin in ref 33. Water molecules would be placed above the alkane regions shown. The probe molecules (ovals) can be adsorbed in an “in” or “out” orientation at the rough interfaces, resulting in unique interfacial polarities for all three surfaces.

$$\text{rough-in-CH}_3 < \text{smooth-CH}_3 < \text{rough-out-CH}_3$$

All systems containing chlorine (rough-in, rough-out, and smooth) were more polar than the alkane systems. From this hierarchy one sees that the polarity scales with a solute’s solvent accessible area. Not surprisingly, greater exposure to the aqueous phase leads to a more polar interfacial environment.

These findings can, in part, be used to interpret the results shown in Figures 7 and 8. At the water/alkane interface each solvent will pack in a way that is determined by its molecular structure. On the basis of its compact geometry, small surface area, and relatively high melting point, we expect the symmetric cyclohexane solvent at the interface to arrange itself in a manner more ordered than in bulk. In fact, this surface-enhanced density has been proposed as the origin of nonadditive solvent polarity at solid/liquid interfaces,[30] and such a surface-induced structure in the organic phase is likely to resemble the “smooth” interface simulated by Vieceli and Benjamin.

The additional methyl group on m-cyclohexane breaks the symmetry found in cyclohexane and creates additional volume between molecules. Additional “free volume” could allow the molecular ruler probe to be more easily solvated in the organic phase. This picture of the interface resembles the “rough-in” interface in the molecular dynamics simulations carried out by Vieceli and Benjamin. In effect, the probe is less exposed to the solvating influence of water, and simulations predict that the “rough-in” interface is less polar than the “smooth” interface. The spectra in Figures 3 and 4 support this picture, with the chromophore of the shortest ruler (C_2) sampling alkane-like solvation at the water/m-cyclohexane interface, but an intermediate polarity at the water/cyclohexane interface. For the water/cyclohexane system polarity across the well-ordered “smooth” interface converges to that of bulk cyclohexane on a longer length scale than for the “rough” water/m-cyclohexane system. These geometric considerations provide a strong motivation to further characterize these interfaces structurally using techniques such as sum frequency generation (SFG) and X-ray and neutron scattering. SFG can report on absolute orientation of solvent species and the degree of solvation at different liquid/liquid interfaces.[31,32] X-ray reflectivity studies may observe the transition from water to alkane manifested as an abrupt exponential decay in reflectivity for sharp interfaces and a more gradual decay for broader interfaces. Information about solvent orientation and conformation at liquid/liquid interfaces will allow further refinement of models of interfacial solvation.

2. Linear Alkanes. Similar to the cyclic alkanes studied, one of the linear alkanes (octane) created a sharper interface than the other (hexadecane). The spectra in Figures 5 and 6 indicate that solvent polarity converges from an intermediate polarity to that of the bulk alkane more abruptly at the water/octane interface than at the water/hexadecane interface. We begin by noting that Schlossman and co-workers examined a number of water/*n*-alkane interfaces using X-ray reflectivity to measure the density profile the interfacial region. Their work focused on linear alkanes and found that as alkane chain length increased, the interfacial width increased. Although the widths reported in these scattering studies measure a different physical property (solvent density) than the one measured in this work (solvent polarity), both sets of results *are* internally consistent. X-ray reflectivity studies measure interfacial width as a function of the density profile across an interface and describe how rapidly the solvent density converges from bulk water to bulk alkane. The interfacial density reflects the physical composition of the interface. In our studies, the interfacial width is a function of the electronic forces between the solute and its surroundings at the boundary between adjacent phases. Nevertheless, despite the differences between the quantities probed by these two experimental techniques, we find it encouraging that the results presented here agree with those from previous studies.

For the data shown in Figures 5 and 6, differences in solvent molecular structure again suggest why octane and hexadecane create different interfacial environments. Solvent packing is an important factor in the ability of octane and hexadecane to solvate the probe. The molecular volume of hexadecane is 488 $Å^3$, and that of octane is 271 $Å^3$. Obviously, hexadecane is larger than octane, but it is not twice as large. In fact, the molecular volume of hexadecane is only 90% of that of two octane molecules. This discrepancy arises from hexadecane's additional conformational flexibility relative to octane. Due to its longer length, hexadecane can bend and adopt more compact conformations. At an interface, these efficient, space-filling geometries mean less free volume to solvate the probe of adsorbed molecular rulers. The interface created by hexadecane compared to octane may be similar to that of cyclohexane compared to m-cyclohexane. As in the case of the cyclic alkanes, we would expect solvents possessing less free volume to produce broader interfaces.

V. Conclusion

We have used molecular rulers to probe solute excitation at several weakly associating water/alkane liquid/liquid interfaces. The data suggest that all these interfaces are sharp, featuring an abrupt transition ($<$9 Å) from the aqueous to the organic phase. However, our findings suggest that some weakly associating interfaces are sharper than others. Differences in dipolar width depend sensitively on solvent structure and appear to correlate with free volume within the organic phase. These findings agree well with predictions from molecular dynamics simulations predicting that interfacial solvent polarity should scale with a solute's solvent accessible area. Ongoing studies will continue to explore the relationship between solvent molecular structure and interfacial width.

Acknowledgment. This work was supported by the Research Corporation (RI0362) and the National Science Foundation through its CAREER Program (CHE0094246).

References and Notes

(1) Volkov, A. G.; Deamer, D. W.; Tanelian, D. L.; Markin, V. S. *Liquid Interfaces in Chemistry and Biology*; John Wiley & Sons: New York, 1998.
(2) Volkov, A. G., Ed. *Liquid Interfaces in Chemical, Biological, and Pharmaceutical Applications*; Marcel Dekker: New York, 2001; Vol. 95.
(3) Chhabra, V.; Free, M. L.; Kang, P. K.; Truesdail, S. E.; Shah, D. O. *Tenside, Surfactants, Deterg.* **1997**, *34*, 156.
(4) Safran, S. A. *Statistical Thermodynamics of Surfaces, Interfaces, and Membranes*; Addison-Wesley: Reading, MA, 1994; Vol. 90.
(5) Chipot, C.; Wilson, M. A.; Pohorille, A. *J. Phys. Chem. B* **1997**, *101*, 782.
(6) Sangster, J. *Octanol−Water Partition Coefficients*; John Wiley and Sons: New York, 1997; Vol. 2.
(7) Mitrinovic, D.; Tikhonov, A. M.; Li, M.; Huang, Z.; Schlossman, M. L. *Phys. Rev. Lett.* **2000**, *85*, 582.
(8) Stanners, C. D.; Du, Q.; Chin, R. P.; Cremer, P.; Somorjai, G. A.; Shen, Y.-R. *Chem. Phys. Lett.* **1995**, *232*, 407.
(9) Tikhonov, A. M.; Mitrinovic, D. M.; Li, M.; Huang, Z.; Schlossman, M. L. *J. Phys. Chem. B* **2000**, *104*, 6336.
(10) Girault, H. H.; Tamburello-Luca, A. A.; Hebert, P.; Brevet, P. F. *J. Chem. Soc., Faraday Trans.* **1996**, *92*, 3079.
(11) Eisenthal, K. B. *J. Phys. Chem.* **1996**, *100*, 12997.
(12) Kitamura, N.; Ishizaka, S.; Kim, H. *Anal. Chem.* **2001**, *73*, 2421.
(13) Steel, W. H.; Walker, R. A. *Nature* **2003**, *424*, 296.
(14) Steel, W. H.; Damkaci, F.; Nolan, R.; Walker, R. A. *J. Am. Chem. Soc.* **2002**, *124*, 4824.
(15) Beildeck, C. L.; Steel, W. H.; Walker, R. A. *Langmuir* **2003**, *19*, 4933.
(16) Schlossman, M. L.; Li, M.; Mitrinovic, D. M.; Tikhonov, A. M. *High Perform. Polym.* **2000**, *12*, 551.
(17) Michael, D.; Benjamin, I. *J. Phys. Chem. B* **1998**, *102*, 5145.
(18) Penfold, J.; Richardson, R. M.; Zarbakhsh, A.; Webster, J. R. P. *J. Chem. Soc., Faraday Trans.* **1997**, *93*, 3899.
(19) Wirth, M. J.; Burbage, J. D. *J. Phys. Chem.* **1992**, *96*, 9022.
(20) Sassaman, J. L.; Wirth, M. J. *Colloids Surf., A* **1994**, *93*, 49.
(21) Kovaleski, J. M.; Wirth, M. J. *J. Phys. Chem.* **1995**, *99*, 4091.
(22) Wang, H.; Borguet, E.; Eisenthal, K. B. *J. Phys. Chem. A* **1997**, *101*, 713.
(23) Wang, H.; Borguet, E.; Eisenthal, K. B. *J. Phys. Chem. B* **1998**, *102*, 4927.
(24) Piron, A.; Brevet, P. F.; Girault, H. H. *J. Electroanal. Chem.* **2000**, *483*, 29.
(25) Steel, W. H.; Walker, R. A. *J. Am. Chem. Soc.* **2003**, *125*, 1132.
(26) Zhang, X.; Esenturk, O.; Walker, R. A. *J. Am. Chem. Soc.* **2001**, *123*, 10768.
(27) Englin, B. A.; Plate, A. F.; Tugolukov, V. M.; Pryanishnikova, M. A. *Chem., Technol. Fuel Oil* **1965**, *10*, 722.
(28) Michael, D.; Benjamin, I. *J. Chem. Phys.* **2001**, *114*, 2817.
(29) Weeks, J. D. *J. Chem. Phys.* **1977**, *67*, 3106.
(30) Zhang, X.; Cunningham, M. M.; Walker, R. A. *J. Phys. Chem. B* **2003**, *107*, 3183.
(31) Scatena, L. F.; Brown, M. G.; Richmond, G. L. *Science* **2001**, *292*, 908.
(32) Scatena, L. F.; Richmond, G. L. *J. Phys. Chem. B* **2001**, *105*, 11240.
(33) Vieceli, J.; Benjamin, I. *J. Phys. Chem. B* **2002**, *106*, 7898.